sustainability

MDPI

Article

Experimental Study on Solidification of Pb^{2+} in Fly Ash-Based Geopolymers

Fang Liu [1], Ran Tang [1], Baomin Wang [2,*] and Xiaosa Yuan [1]

[1] Shaanxi Key Laboratory of Safety and Durability of Concrete Structures, Xijing University, Xi'an 710123, China; liufang_winter@163.com (F.L.); tangran627@163.com (R.T.); yuanxiaosa2009@163.com (X.Y.)
[2] School of Civil Engineering, Dalian University of Technology, Dalian 116023, China
* Correspondence: wangbm@dlut.edu.cn; Tel.: +86-0411-8470-7101

Abstract: Fly ash from the incineration of domestic waste contains heavy metals, which is harmful to the environment. To reduce and prevent their contamination, heavy metal ions need to be sequestered. In this study, the geopolymer prepared by fly ash, a kind of power plant waste, is used to cure the heavy metal Pb^{2+}, and to investigate the effect of different concentrations of Pb^{2+} on the compressive strength of the solidified body at different ages; the curing effect is judged by the toxic leaching concentration of heavy metals; the resistance of the solidified body to immersion is evaluated by comparing the change in strength before and after leaching; the fly ash-based geopolymer solidified body is compared with the cement solidified body in terms of curing effectiveness; the properties of the geopolymer and its mechanism of curing heavy metals are explored by microscopic tests. The results show that the fly ash-based geopolymer solidified body has good resistance to immersion; the optimum curing concentration of Pb^{2+} in fly ash-based geopolymers is 2.0%; compared to pure geopolymers, the strength of the solidified body at 28 d decreases by only 13.0%, and the leaching concentration of Pb^{2+} is 4.73 $mg \cdot L^{-1}$, which meets the specification requirements; the curing effect of the fly ash-based geopolymer is better than the cement solidified body; the microscopic test results indicate that the curing of Pb^{2+} by the fly ash-based geopolymer is a combination of both chemical bonding and physical fixation.

Keywords: fly ash; geopolymer; solidification; heavy metal; leaching concentration

Citation: Liu, F.; Tang, R.; Wang, B.; Yuan, X. Experimental Study on Solidification of Pb^{2+} in Fly Ash-Based Geopolymers. *Sustainability* **2021**, *13*, 12621. https://doi.org/10.3390/su132212621

Academic Editors: Carlos Morón Fernández and Daniel Ferrández Vega

Received: 20 October 2021
Accepted: 12 November 2021
Published: 15 November 2021

1. Introduction

With the development of society, the discharge of domestic waste increases rapidly. Proper disposal of these wastes has become an important task. At present, there are three common methods: landfilling, composting, and incineration [1], of which incineration is becoming the main method because of its high efficiency, speed, significant volume reduction, and the possibility of converting waste into other energy sources; however, after waste incineration, most of the heavy metals such as Pb, Cr, and Zn will go into the fly ash that can cause irreversible damage to the environment and humans if handled improperly.

An important means of dealing with heavy metal waste is to cure them to reduce or even prevent their contamination. The solidified cement is commonly used for this purpose, but it has obvious drawbacks, including high concentrations of toxic leaching of heavy metals, poor durability, and poor resistance to acidic soils and rainfall [2,3].

The geopolymer [4] is a new type of inorganic polymeric material with high strength and durability. It is prepared by the polymerization of silica-aluminous raw materials, such as metakaolin [5,6], slag [7], kaolinite [8], and fly ash [9,10], under the solubilization of alkali activator to form an amorphous silica-aluminum compound. Andini, S. [11] investigated the effect of different curing temperatures on the performance of geopolymers synthesized from fly ash, and determined the optimum curing temperature. Duxson, P. [12] studied the mechanical properties of geopolymer with different types of alkali activators

and different silica-aluminum ratios in relation to age, and found that the sodium alkali activator is more effective than the potassium alkali activator in stimulating geopolymers.

The internal structure of geopolymers exhibits a three-dimensional mesh-like structure similar to that of zeolites that makes it uniquely suited to the solidification of almost all heavy metal ions [13–16].

As reported in [17,18], geopolymers can efficiently bind heavy metals in their matrix structure; the reaction mechanism could be physical or chemical bonding. Studies by Van Jaarsveld et al. [19] suggested that Pb might be chemically bonded within the aluminosilicate matrix, but the exact form was unclear. In contrast, Palacios and Palomo [20] suggested that Pb was solidified to insoluble Pb_3SiO_5 in NaOH-activated fly ash cementitious materials.

Therefore, a geopolymer was prepared using waste fly ash as a matrix in this study to investigate its curing of heavy metals and the mechanism. Additionally, the heavy metal Pb^{2+} was solidified through the geopolymer to study the effect of its concentration on the compressive strength of the solidified body at different ages, and on the toxic leaching concentration of heavy metals, and to compare the curing effect of the fly ash-based geopolymer with that of the cement solidified body. Furthermore, the properties of the geopolymer and its mechanism of curing heavy metals were explored through microscopic tests (XRD, FT-IR, and SEM) to investigate the reaction process, structural morphological changes, and curing mechanisms at a microscopic level.

2. Raw Materials and Experimental Procedures

2.1. Raw Materials

2.1.1. Fly Ash

The ultra-fine fly ash used in this study came from Guodian Zhuanghe power plant in Liaoning Province. The chemical composition of this fly ash is given in Table 1, and its main technical indicators are listed in Table 2.

Table 1. Chemical composition of fly ash.

SiO_2	Al_2O_3	Fe_2O_3	CaO	TiO_2	K_2O	MgO
48.67%	29.16%	8.98%	4.73%	2.75%	2.66%	0.74%

Table 2. Summary of main technical indicators of fly ash.

Item	Test Result	Standard of Class I Fly Ash
Water content	0.72%	≤1%
Water requirement ratio	93.8%	≤95%
Fineness	2.3%	≤12%
Strength activity index	78.1%	≥70%

2.1.2. Water Glass

The sodium water glass ($Na_2O{\cdot}nSiO_2$) was obtained from Usolf Chemical Technology Co., Ltd. in Shandong Province. The specific parameters are listed in Table 3.

Table 3. Relevant parameters of water glass.

Name	Content
Na_2O	8.3%
SiO_2	26.5%
H_2O	65.2%
Modulus	3.3
Appearance	Transparent and viscous liquid

2.1.3. Other Raw Materials and Chemical Reagents

(1) NaOH

It was analytical pure level that was used to adjust the modulus of the water glass to configure a compound alkali activator required for the experiment.

(2) H_2SO_4, HNO_3

They were analytical pure levels that were used to prepare leaching solutions in simulated acidic environments, and to leach fly ash-based geopolymer samples in preparation for subsequent heavy metal leaching concentration tests.

(3) Heavy metal salt

The aim of this study is to research the solidification of Pb^{2+}; therefore, nitrate ($Pb(NO_3)_2$, analytical pure level) was chosen to avoid the interference of anions in heavy metal salts.

(4) Water

The deionized water used in this test was supplied by Bonuo Chemical Reagent Factory.

2.2. Preparation of the Fly Ash-Based Geopolymer

In this test, Pb^{2+} was introduced in the form of $Pb(NO_3)_2$, while its content (in terms of mass of Pb^{2+} as a percentage of solid mass) was set at six levels of 0.5%, 1.0%, 1.5%, 2.0%, 2.5%, and 3.0%, respectively. The experimental ratios of materials used for the fly ash-based geopolymer are listed in Table 4.

Table 4. Material proportioning for fly ash-based geopolymer solidified body.

No.	Fly Ash/g	Water Glass/g	NaOH/g	Water/g	$Pb(NO_3)_2$/g	Pb^{2+} Content/%
1	1000.00	299.17	47.80	104.94	8.00	0.50
2	1000.00	299.17	47.80	104.94	15.99	1.00
3	1000.00	299.17	47.80	104.94	23.99	1.50
4	1000.00	299.17	47.80	104.94	31.98	2.00
5	1000.00	299.17	47.80	104.94	39.98	2.50
6	1000.00	299.17	47.80	104.94	47.97	3.00

According to Table 4, fly ash, water glass, water, and $Pb(NO_3)_2$ were added to the mixing pot of the mechanical mixer in turn, and stirred for 3 min (30 s slow stirring and 1 min fast stirring, repeated, and then finished). Next, the mixture was poured into a 40 × 40 × 40 mm mold, which had been painted in advance with a release agent, and vibrated for 2 min on a vibrating table, before sealing the surface with polyethylene film to prevent moisture evaporation. After standing for 2 h at room temperature, the mold was placed in a high temperature curing box at 65 °C for 24 h before being taken out and demolded, and then it continued to be placed in a standard curing box for closed curing until the age of 3 d, 7 d, and 28 d.

2.3. Analytical Test Methods

2.3.1. Compressive Strength Test

The compressive strength test was performed according to *Method of testing cements—Determination of strength*, GB/T17671-1999.

2.3.2. Leaching Concentration Test for Heavy Metal Ions

The test was performed according to GB5085.3-2007 and GB14569.1-2011. The preparation of the leaching solution required was carried out according to HJ/T299-2007 and HJ557-2010, simulating the acid rain environment and the normal environment, respectively; and then, the leaching concentration of heavy metals was measured by Inductive Coupled Plasma Emission Spectrometer (ICP) test according to GB/T23942-2009.

2.3.3. Microscopic Test

X-ray diffraction (XRD), Fourier-transform infrared spectroscopy (FT-IR), and scanning electron microscopy (SEM) were used to test and analyze the performance of samples of the fly ash-based geopolymer, and the heavy metal ion solidified body on a micromorphological basis.

3. Results and Discussion

3.1. Compressive Strength

The compressive strength and its trends in the curing of Pb^{2+} by the fly ash-based geopolymer are shown in Table 5 and Figure 1.

Table 5. Compressive strength of fly ash-based geopolymer solidified body.

No.	Pb^{2+} Content/%	Compressive Strength at 3 d (Strength Loss)/MPa	Compressive Strength at 7 d (Strength Loss)/MPa	Compressive Strength at 28 d (Strength Loss)/MPa
0	0.0	45.26	46.66	48.72
1	0.5	44.07 (2.6%)	45.73 (2.0%)	47.84 (1.8%)
2	1.0	42.96 (5.1%)	44.47 (4.7%)	46.67 (4.2%)
3	1.5	40.25 (11.1%)	41.99 (10.0%)	44.82 (8.0%)
4	2.0	37.54 (17.1%)	39.67 (15.0%)	42.39 (13.0%)
5	2.5	33.79 (25.3%)	36.86 (21.0%)	39.46 (19.0%)
6	3.0	27.38 (39.5%)	29.40 (37.0%)	31.67 (35.0%)

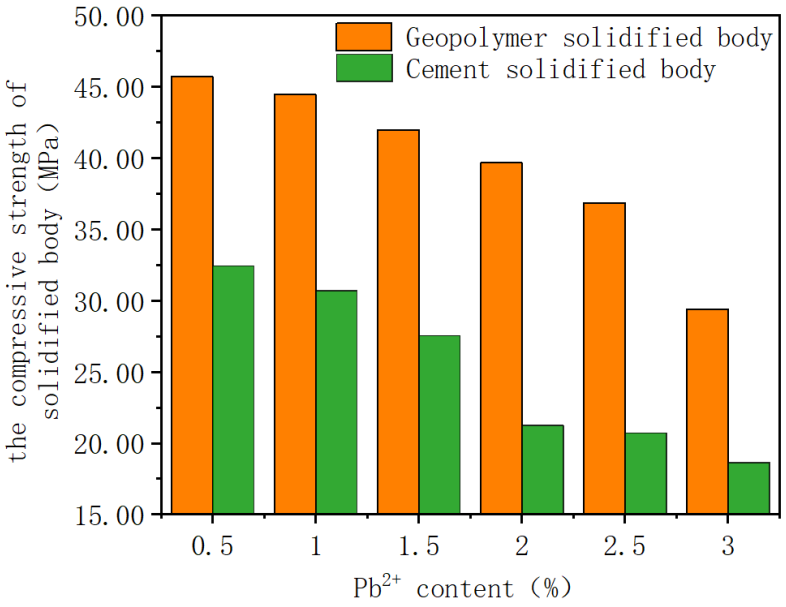

Figure 1. Comparison of the compressive strength of the geopolymer and the cement solidified body.

According to Table 5, the compressive strength of the fly ash-based geopolymer at each age decreases gradually with the increase in Pb^{2+} concentration. Additionally, at the same Pb^{2+} concentration, the internal reaction of the geopolymer is gradually complete, and the alkali activator fully acts with the increase of age, corresponding to the increasing strength of the solidified body. It is analyzed that, before Pb^{2+} concentration reaches 2.0%, the compressive strength of the solidified body at 3 d, 7 d, and 28 d can still be maintained at around 40 MPa, with good mechanical properties; after 2.0%, the strength decreases rapidly; when Pb^{2+} reaches 3.0%, the compressive strength at 3 d decreases by nearly 40%. The reason could be that the introduction of Pb^{2+} inhibits the polymerization reaction to some extent, or it has some effect on the internal structure of the solidified body.

3.2. Toxic Leaching Concentration of Heavy Metals

3.2.1. Neutral Environment

According to Table 6, in a neutral environment, the toxic leaching concentration of heavy metals in the fly ash-based geopolymer solidified body increases with the increase of Pb^{2+} content. At the same heavy metal concentration, the polymerization reaction within the solidified body tends to be thorough with the increase in age; its internal cage-like sequestration structure is more complete; the sequestration effect on heavy metal ions is more effective; the leaching concentration of the heavy metal solidified body decreases accordingly. When the heavy metal content is 2.5%, the leaching concentrations of the solidified body at 3 d and 7 d exceed the specification maximum limit (5 $mg \cdot L^{-1}$), while the concentration at 28 d does not; when the heavy metal content reaches 3%, the leaching concentration of the solidified body at 28 d is only above the limit. Therefore, the optimum Pb^{2+} content ranges from 2% to 2.5% in a neutral environment.

Table 6. Results of toxic leaching concentration corresponding to different Pb^{2+} contents in a neutral environment.

No.	Pb^{2+} Content/%	Leaching Concentration of Heavy Metals in Solidified Body/$mg \cdot L^{-1}$		
		3 d	7 d	28 d
1	0.5	1.05	0.81	0.53
2	1.0	1.67	1.34	1.03
3	1.5	3.53	3.09	2.82
4	2.0	4.26	3.79	3.35
5	2.5	5.38	5.03	4.87
6	3.0	6.42	5.89	5.24

3.2.2. Acid Environment

As shown in Table 7, the toxic leaching pattern of heavy metals in an acid environment is generally the same as that in a neutral environment; however, the external and internal structure of the solidified body is more significantly attacked by the acid environment than the neutral environment, so that heavy metal ions are more likely to migrate out of the internal structure of the geopolymer, resulting in higher leaching concentrations for each Pb^{2+} content and each age of the solidified body in an acid environment than in a neutral environment.

Table 7. Results of toxic leaching concentrations corresponding to different Pb^{2+} contents in an acid environment.

No.	Pb^{2+} Content/%	Leaching Concentration of Heavy Metals in Solidified Body/$mg \cdot L^{-1}$		
		3 d	7 d	28 d
1	0.5	1.25	1.12	0.89
2	1.0	1.93	1.72	1.46
3	1.5	4.06	3.95	3.35
4	2.0	4.93	4.89	4.73
5	2.5	6.31	6.02	5.47
6	3.0	8.36	7.97	7.61

When Pb^{2+} reaches 2%, the leaching concentrations of the solidified body at the ages of 3 d, 7 d, and 28 d are close to the normative limit, but does not yet exceed it, while at the Pb^{2+} content of 2.5%, the limit is exceeded at all ages. To sum up, the optimum solidifying concentration range for Pb^{2+} in the fly ash-based geopolymer in an acid environment is similarly between 2% and 2.5%.

3.3. Immersion Resistance

Two groups of fly ash-based geopolymer solidified body with different Pb^{2+} doping are set. One group is used as a control group to test the strength before immersion; the other is placed in a water tank at room temperature and is flooded over the surface. The specimens are removed and dried with a rag after being immersed for 90 days, and then, they are tested for the compressive strength. Test results are listed in Table 8.

Table 8. Changes of the strength before and after immersion.

No.	Pb^{2+} Content/%	Strength before Immersion/MPa	Strength after Immersion/MPa	Strength Loss/%
1	0.5	47.84	36.31	24.10
2	1.0	46.67	37.98	18.62
3	1.5	44.82	34.59	22.82
4	2.0	42.39	35.82	15.50
5	2.5	39.46	29.65	24.85
6	3.0	31.67	21.97	30.63

According to Table 8, the strength loss of the solidified body does not exceed the limit of 25% for each Pb^{2+} content, except for the highest content (3.0%). Therefore, it can be concluded that the fly ash-based geopolymer solidified body has good resistance to soaking.

3.4. Comparison between the Fly Ash-Based Geopolymer and the Cement Solidified Body

To verify the effectiveness of the fly ash-based geopolymer in solidifying Pb^{2+}, the cement solidified body is chosen for comparison in this study. Both are set to the same water to ash ratio, and the same amount of Pb^{2+} (0.5%, 1.0%, 1.5%, 2.0%, 2.5%, and 3.0%). The compressive strength of the solidified body at 7 d, and the toxic leaching concentrations at 28 d (acid environment) are used as indicators to compare the solidifying effect of these two. The experimental results are shown in Figures 1 and 2.

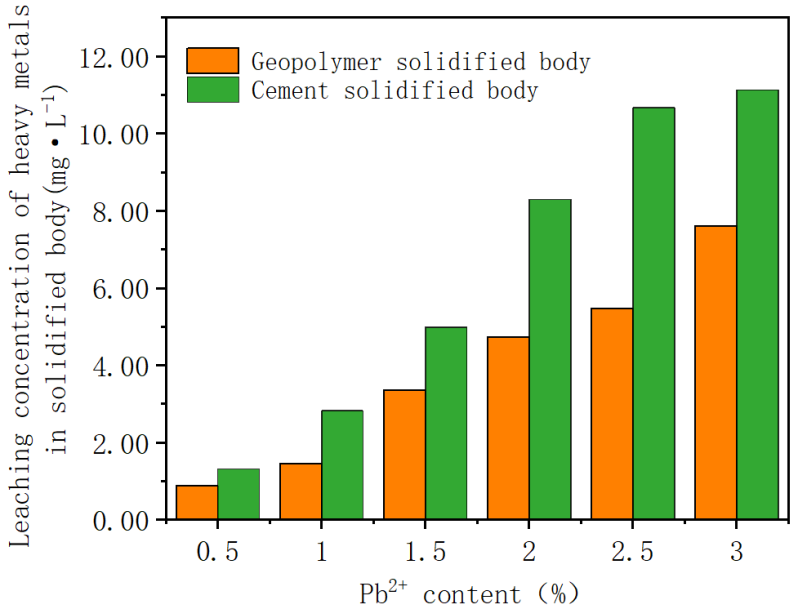

Figure 2. Comparison of heavy metal leaching concentration of geopolymer and cement solidified body.

As shown in Figure 1, the compressive strength of the fly ash-based geopolymer solidified body is significantly higher than that of the cement solidified body. It is analyzed

that the compressive strengths of both tend to decrease with the increase in Pb^{2+} content. When Pb^{2+} concentration is 2%, the compressive strength of the geopolymer solidified body is still around 40 MPa; the strength decreases slowly until the Pb^{2+} concentration reaches 2%, and more rapidly after this. In contrast, the strength of the cement solidified body decreases at a relatively rapid rate all along. Therefore, the performance of the geopolymer solidified body is significantly better from the point of view of the compressive strength.

According to Figure 2, in an acid environment, the solidification of Pb^{2+} in the fly ash-based geopolymer solidified body is better than in the cement solidified body. At 2% Pb^{2+}, the leaching concentration of the geopolymer solidified body is still below 5 $mg \cdot L^{-1}$, the limit value for Pb^{2+} is specified in GB5085.3-2007, whereas the cement solidified body is very close to the normative limit at 1.5% Pb^{2+}.

This is mainly due to that in an acid environment, the hydration products of cement, such as C-S-H (calcium silicate hydrate) and $Ca(OH)_2$, react with the acid to produce the corresponding calcium salts, resulting in an increase in pore space within the solidified body, which ultimately leads to the destruction of the solidified body and a reduction in its solidifying ability. By comparison, the silicon–oxygen (Si-O) and aluminum–oxygen (Al-O) bonded in the internal structure of the geopolymer are difficult to break in an acid environment, making it more resistant to acid attack.

To sum up, whether from the point of view of mechanical properties (compressive strength) or solidifying properties (leaching concentration), the performance of the fly ash-based geopolymer solidified body is better than that of the cement solidified body.

3.5. Solidifying Mechanism Analysis

3.5.1. XRD

The XRD pattern of the fly ash used for the test is shown in Figure 3. It can be seen that the main body of the fly ash is amorphous, and its crystalline substances are quartz and mullite, which are the main substances containing silicon and aluminum. The characteristic peaks of quartz appear at 22.53°, 50.71°, and 54.69°; and that of mullite at 17.15°, 27.33°, 32.67°, and 34.82°. The diffraction peaks in a "bun" shape in the 2θ angle range of 15° to 30° indicate the presence of vitreous body in the fly ash, from which the activity of the fly ash is mainly derived.

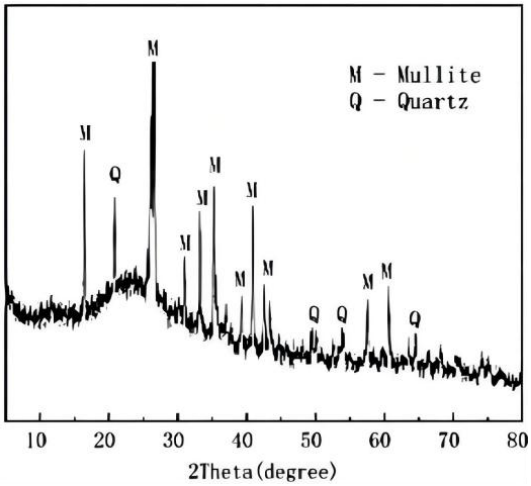

Figure 3. XRD pattern of fly ash.

The variations in the mineral phase of the fly ash-based geopolymer and its solidified body are shown in Figure 4. Comparing Figure 4 with Figure 3, the crystalline phases in the fly ash-based geopolymer are mainly mullite and quartz, with a small amount of calcium silicate present at 39.54°, and the crystalline diffraction peaks are somewhat reduced compared to that in the fly ash XRD pattern, demonstrating that the crystalline substances in the fly ash react to form amorphous substances during the alkali excitation

process. Additionally, in the curve of the pure fly ash-based geopolymer, "bun"-shaped dispersion peaks appear in the interval 18° to 35 °, which are slightly shifted to the right compared to the fly ash curve, indicating that the dissolution of the vitreous body in the fly ash produces amorphous gel-like substance in the fly ash-based geopolymer; the absence of new phases and the disappearance of old phases mean that some of the crystalline particles in the fly ash are dissolved, and some are encapsulated by the gel material in the geopolymer, which corresponds to the SEM results.

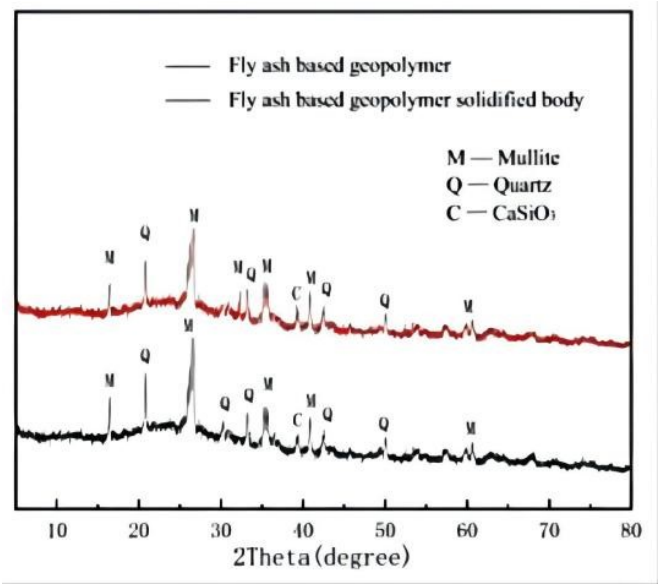

Figure 4. XRD pattern of the fly ash-based geopolymer and its solidified body.

Compared to the curve in Figure 3, the overall curve in Figure 4 is flatter, which means a relatively high degree of reaction, and a more adequate polymerization of the silica-aluminous material in the raw material with the alkali activator, resulting in a good strength of the geopolymer. Diffraction peaks of crystalline minerals associated with Pb^{2+} are not found on the curve of the solidified body doped with Pb^{2+}, and no new phases appear, which means that Pb^{2+} is not involved in the overall internal chemistry of the geopolymer and the Pb_3SiO_5 phase suggested by Palomo et al. [20] is not detected. It can be assumed that Pb^{2+} may have been bonded to the internal structural skeleton of the fly ash-based geopolymer, or the solidification of heavy metal ions by the geopolymer solidified body is a physical encapsulation.

3.5.2. SEM

Figure 5a shows a micrograph of the fly ash-based geopolymer in the early stage of the reaction. At this stage, the fly ash particles have not fully reacted; half of them are dissolved, while the other half appears partially encapsulated on the surface.

Figure 5b shows a micrograph of the fly ash-based geopolymer at a later stage of the reaction. It can be observed that the fly ash, after polymerization with the alkali activator, produces a very dense geopolymer gel (silica-aluminate gel) with a uniformly dense and amorphous outer surface; the particles in the fly ash are completely dissolved or encapsulated within the formed geopolymer gel; the beads are no longer visible compared to the pre-reaction period, but traces of their internal concavity left by the dissolution reaction can be found. Overall, the internal morphology of the fly ash-based geopolymer is dominated by a dense amorphous structure, which means that the reaction of the materials in this test is sufficient and the polymerization reaction of internal depolymerization and polycondensation is complete. As a result, the fly ash-based geopolymer obtained from the reaction possesses good physicochemical properties.

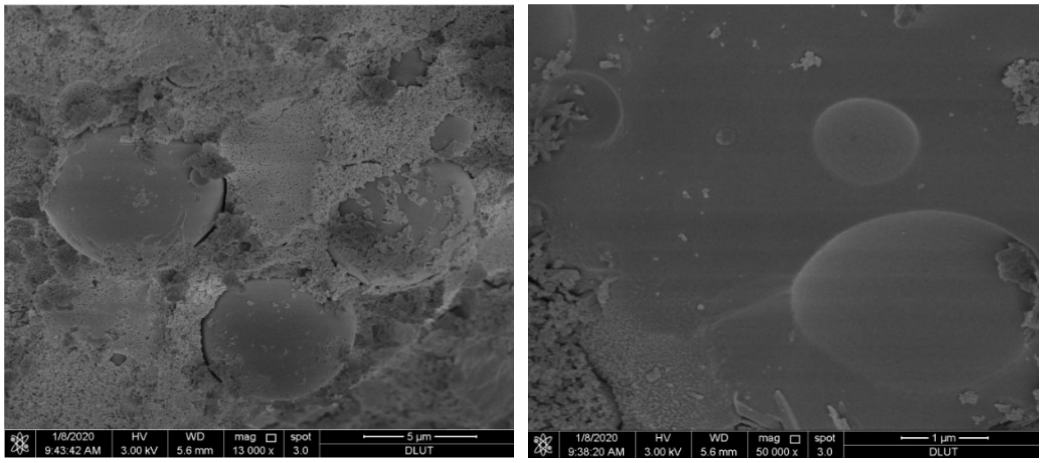

(**a**) Early stage (**b**) Later stage

Figure 5. SEM of the fly ash-based geopolymer in the early and later stages of the reaction.

Figure 6 shows the electron micrographs of the fly ash-based geopolymer during the reaction. Compared to the early stage of the reaction in Figure 5a, the wrapping condition in Figure 6a is more complete, and the progress of the reaction can be clearly observed. Figure 6b is a partial magnification, showing that the gel in the geopolymer slowly grows and extends from the top of the particle downwards until it completely wraps around the geopolymer, forming a kind of core-shell structure. These indicate that a portion of the fly ash particles is encapsulated by the gel into a core-shell structure, except for a portion being dissolved by the alkaline solution. The outer shell of this structure extends until it completely encapsulates the geopolymer and then forms a integral whole with its surrounding dense gel-like substances, which also has a beneficial effect on the mechanical properties of the geopolymer.

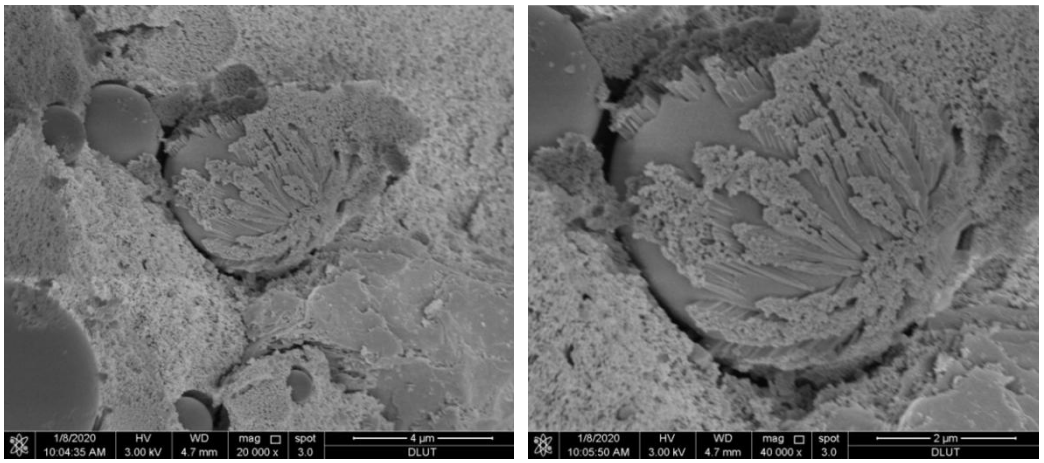

(**a**) Before magnification (**b**) After magnification

Figure 6. SEM of the fly ash-based geopolymer during the reaction.

Figure 7a shows the state during the solidifying Pb^{2+} reaction of the fly ash-based polymer, and the fully reacted state is given in Figure 7b. Compared to Figure 7a, a more complete and dense whole is formed in the latter figure, resulting in a good performing solidified body of the fly ash-based geopolymer.

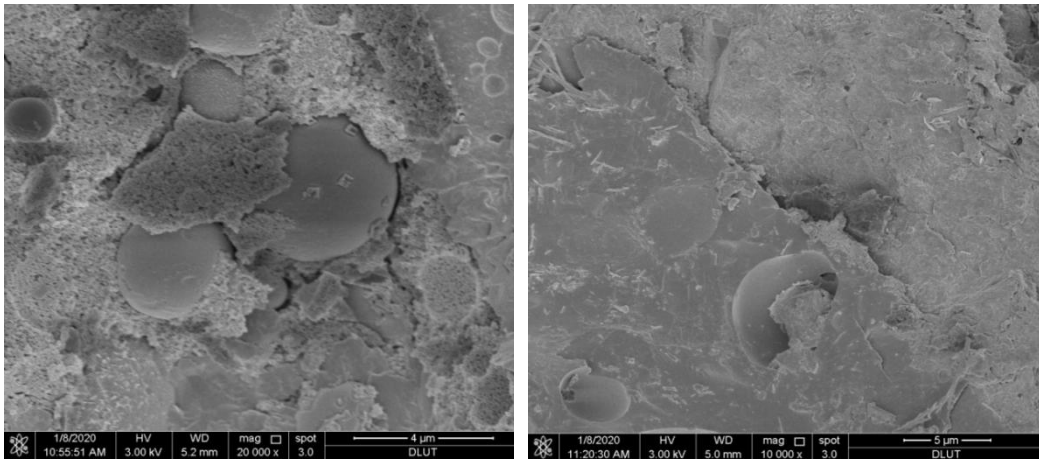

(**a**) During reaction (**b**) After reaction

Figure 7. SEM of Pb^{2+} solidified body of the fly ash-based geopolymer.

3.5.3. FT-IR

The infrared spectrum of the fly ash-based geopolymer and its solidified body is shown in Figure 8.

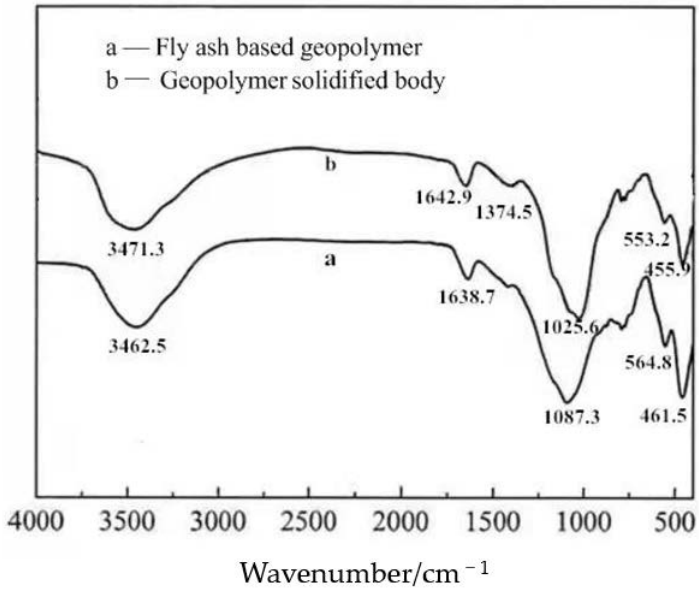

Figure 8. Infrared spectrum of the fly ash-based geopolymer and its solidified body.

According to the figure, the geopolymer exhibits O-H stretching vibration and O-H bending vibration at 3462.5 cm^{-1} and 1638.7 $cm^{-1,}$ respectively; while the solidified body exhibits O-H stretching vibration and O-H bending vibration at 3471.3.4 cm^{-1} and 1642.9 cm^{-1}, respectively, which is surmised to be due to the presence of bound water within the geopolymer and the solidified body. The absorption peaks at 1087.3 cm^{-1} of the geopolymer and 1025.6 cm^{-1} of the solidified body in the infrared spectrogram correspond to the stretching vibration of Si-O-T (T = Si or Al). The introduction of Pb^{2+} has an effect on the stretching vibrations of Si-O-T around 1087.3 cm^{-1} in the geopolymer, indicating that it is bonded into the backbone of the geopolymer. The absorption peaks near 564.8 cm^{-1} of the geopolymer and 553.2 cm^{-1} of the solidified body correspond to the stretching vibration of Al-O-Si. The bending vibration of Si-O or Al-O of the geopolymer and its solidified body is located near 461.5 cm^{-1} and 455.9 cm^{-1}, respectively. The peak at 1374.5 cm^{-1} occurs only in the solidified body, which is analyzed as being due to the nitrate

contained in the heavy metal salts when Pb^{2+} is introduced. Overall, the infrared spectrum of the two samples is generally consistent, with no significant differences in the positions of the individual absorption peaks, indicating that the main structure of the solidified body is a complex three-dimensional mesh structure formed by the polymerization of silica-oxygen and aluminum-oxygen tetrahedra, although there are some differences in its physicochemical properties after the introduction of Pb^{2+}.

4. Conclusions

In this study, the fly ash-based geopolymer was prepared to solidify Pb^{2+}; the mechanical properties and leaching concentration of fly ash-based geopolymer were studied; the effects of different concentrations of Pb^{2+} on the compressive strength and solidifying effect of the solidified body were analyzed, and were compared with the cement solidified body; the reaction process, structural morphology, and solidifying mechanism were studied by XRD, FT-IR and SEM. The main conclusions are as follows:

(1) The compressive strength of the solidified body decreases compared to that of the pure geopolymer; the higher the concentration of Pb^{2+} added, the greater the decrease in strength. The solidifying performance of the fly ash-based geopolymer solidified body in a neutral environment is better than that in an acidic environment. Taking into account the compressive strength and leaching concentration, the optimum solidifying concentration of Pb^{2+} in the fly ash-based geopolymer is 2.0%.

(2) The fly ash-based geopolymer solidified body performs better than the cement solidified body, in terms of both mechanical properties (the compressive strength) and solidifying properties (leaching concentration). At Pb^{2+} concentration of 2%, the compressive strength of the geopolymer solidified body can still reach around 40 MPa and its leaching concentration is below the limit, whereas the compressive strength of the cement solidified body is only 21.25 MPa, and the leaching concentration is already as high as 8.29 $mg \cdot L^{-1}$.

(3) The analysis of the mineral composition, microscopic morphology, and chemical structure of the fly ash-based geopolymer and its solidified body by XRD, SEM and FTIR reveals that the fly ash-based geopolymer forms a complete whole inside with a very dense structure, and possesses good physicochemical properties. The solidifying of Pb^{2+} by the geopolymer is a combination of both chemical bonding and physical encapsulation.

Author Contributions: Data curation and investigation, R.T.; writing—original draft preparation, F.L.; writing—review and editing, X.Y.; supervision, B.W. All authors have read and agreed to the published version of the manuscript.

Funding: This work is supported by the National Natural Science Foundation of China [51878116 and 51902270]; Liaoning Province Key Project of Research and Development Plan [2020JH2/10100016]; Dalian Science and Technology Innovation Fund Project [2020JJ26SN060]; the Youth Innovation Team of Shaanxi Universities.

Institutional Review Board Statement: Not applicable.

Informed Consent Statement: Not applicable.

Data Availability Statement: The data are not to be shared.

Conflicts of Interest: The authors declare no conflict of interest.

References

1. Zhang, Y. The Status and Prediction for Solid Waste Treatment Technology in China. *Environ. Sanit. Eng.* **2000**, *2000*, 81–84. (In Chinese)
2. Bie, R.; Chen, P.; Song, X.; Ji, X. Characteristics of municipal solid waste incineration fly ash with cement solidification treatment. *J. Energy Inst.* **2016**, *89*, 704–712. [CrossRef]
3. Liu, X. Discussion on current treatment and disposal technology situation of MSW fly ash in our country. *Eng. Constr.* **2014**, *46*, 56–60. (In Chinese)
4. Zheng, J.; Qin, W. Research progress of Geopolymer Materials. *New Build. Mater.* **2002**, *2002*, 11–12. (In Chinese)
5. Lancellotti, I.; Kamseu, E.; Michelazzi, M.; Barbieri, L.; Corradi, A.; Leonelli, C. Chemical stability of geopolymers containing municipal solid waste incinerator fly ash. *Waste Manag.* **2010**, *30*, 673–679. [CrossRef] [PubMed]

6. Lizcano, M.; Kim, H.S.; Basu, S.; Radovic, M. Mechanical properties of sodium and potassium activated metakaolin-based geopolymers. *J. Mater. Sci.* **2012**, *47*, 2607–2616. [CrossRef]
7. Ma, S.; Chen, P.; Liu, R. Study on seawater erosion to geopolymeric materials. *New Build. Mater.* **2009**, *36*, 58–61. (In Chinese)
8. Mo, X.; Wang, R.; Pang, J.; Su, F.; Cui, X. Study on preparation and flexural strength of geopolymer based composites materials. *J. Guangxi Univ. (Nat. Sci. Ed.)* **2009**, *34*, 183–186. (In Chinese)
9. Guo, X.; Shi, H.; Dick, W.A. Compressive strength and microstructural characteristics of class C fly ash geopolymer. *Cem. Concr. Compos.* **2010**, *32*, 142–147. [CrossRef]
10. Luna Galiano, Y.; Fernández Pereira, C.; Vale, J. Stabilization/solidification of a municipal solid waste incineration residue using fly ash-based geopolymers. *J. Hazard. Mater.* **2011**, *185*, 373–381. [CrossRef] [PubMed]
11. Andini, S.; Cioffi, R.; Colangelo, F.; Grieco, T.; Montagnaro, F.; Santoro, L. Coal fly ash as raw material for the manufacture of geopolymer-based products. *Waste Manag.* **2008**, *28*, 416–423. [CrossRef] [PubMed]
12. Duxson, P.; Mallicoat, S.; Lukey, G.; Kriven, W.; van Deventer, J. The effect of alkali and Si/Al ratio on the development of mechanical properties of metakaolin-based geopolymers. *Colloids Surf. A Physicochem. Eng. Asp.* **2007**, *292*, 8–20. [CrossRef]
13. Bankowski, P.; Zou, L.; Hodges, R. Using inorganic polymer to reduce leach rates of metals from brown coal fly ash. *Miner. Eng.* **2004**, *17*, 159–166. [CrossRef]
14. Zhang, J.; Provis, J.L.; Feng, D.; van Deventer, J.S. Geopolymers for immobilization of Cr^{6+}, Cd^{2+}, and Pb^{2+}. *J. Hazard. Mater.* **2008**, *157*, 587–598. [CrossRef] [PubMed]
15. Provis, J.L.; Rose, V.; A Bernal, S.; van Deventer, J.S.J. High-Resolution Nanoprobe X-ray Fluorescence Characterization of Heterogeneous Calcium and Heavy Metal Distributions in Alkali-Activated Fly Ash. *Langmuir* **2009**, *25*, 11897–11904. [CrossRef] [PubMed]
16. Minarikova, M.; Skvara, F. Fixation of heavy metals in geopolymeric materials based on brown coal fly ash. *Ceram. Silik.* **2006**, *50*, 200–207.
17. Singh, R.; Budarayavalasa, S. Solidifacation and stabilization of hazardous wastes using geopolymers as sustainable binders. *J. Mater. Cycles Waste* **2021**, *23*, 1699–1725. [CrossRef]
18. El-Eswed, B.; Yousef, R.; Alshaaer, M.; Hamadneh, I.; Al-Gharabli, S.; Khalili, F. Stabilization/solidification of heavy metals in kaolin/zeolite based geopolymers. *Int. J. Miner. Process.* **2015**, *137*, 34–42. [CrossRef]
19. van Jaarsveld, J.; van Deventer, J. The effect of metal contaminants on the formation and properties of waste-based geopolymers. *Cem. Concr. Res.* **1999**, *29*, 1189–1200. [CrossRef]
20. Palomo, A.; Palacios, M. Alkali-activated cementitious materials: Alternative matrices for the immobilisation of hazardous wastes: Part II. Stabilisation of chromium and lead. *Cem. Concr. Res.* **2003**, *33*, 289–295. [CrossRef]